

Projection of Extreme Temperatures in Hong Kong in the 21st Century

LEE Tsz-cheung[†](李子祥), CHAN Kin-yu (陈建宇), and GINN Wing-lui (甄荣磊)

Hong Kong Observatory, 134A Nathan Road, Tsim Sha Tsui, Kowloon, Hong Kong

(Received May 7, 2010; revised August 6, 2010)

ABSTRACT

The possible changes in the frequency of extreme temperature events in Hong Kong in the 21st century were investigated by statistically downscaling 26 sets of the daily global climate model projections (a combination of 11 models and 3 greenhouse gas emission scenarios, namely A2, A1B, and B1) of the Fourth Assessment Report of the Intergovernmental Panel on Climate Change. The models' performance in simulating the past climate during 1971–2000 has also been verified and discussed. The verification revealed that the models in general have an acceptable skill in reproducing past statistics of extreme temperature events. Moreover, the models are more skillful in simulating the past climate of the hot nights and cold days than that of the very hot days. The projection results suggested that, in the 21st century, the frequency of occurrence of extremely high temperature events in Hong Kong would increase significantly while that of the extremely low temperature events is expected to drop significantly. Based on the multi-model scenario ensemble mean, the average annual numbers of very hot days and hot nights in Hong Kong are expected to increase significantly from 9 days and 16 nights in 1980–1999 to 89 days and 137 nights respectively in 2090–2099. On the other hand, the average annual number of cold days will drop from 17 days in 1980–1999 to about 1 day in 2090–2099. About 65 percent of the model-scenario combinations indicate that there will be on average less than one cold day in 2090–2099. While all the model-emission scenarios in general have projected consistent trends in the change of temperature extremes in the 21st century, there is a large divergence in the projections between different model/emission scenarios. This reflects that there are still large uncertainties in the model simulation of the future climate of extreme temperature events.

Key words: extreme temperature projections, statistical downscaling, climate projections, climate change, Hong Kong

Citation: Lee Tsz-cheung, Chan Kin-yu, and Ginn Wing-lui, 2011: Projection of extreme temperatures in Hong Kong in the 21st century. *Acta Meteor. Sinica*, **25**(1), 1–20, doi: 10.1007/s13351-011-0001-3.

1. Introduction

The Fourth Assessment Report (AR4) of the Inter-governmental Panel on Climate Change (IPCC) states that warming of the climate system is unequivocal. Most of the observed increases in global average temperature since the mid-20th century are very likely due to the observed increase in anthropogenic greenhouse gas (GHG) concentrations (IPCC, 2007a). Besides the shifting of the mean temperature, the frequency of extreme temperature events (such as heat waves, cold spells, etc.) has also changed in some regions, leading to significant socio-economical impacts (Frich et al., 2002; IPCC, 2007b; WMO, 2009).

For Hong Kong and southern China, the annual mean temperature in the region has a long-term in-

creasing trend under the effect of global warming and urbanization (Leung et al., 2004a; Lee et al., 2006; Guangdong Provincial Meteorological Bureau, 2007; Fong et al., 2009). Recent studies of past occurrences of extreme temperature (Wong and Mok, 2009; Lee et al., 2011) revealed that the extreme daily minimum and maximum temperatures as well as the warm spell duration in Hong Kong exhibit statistically significant long-term rising trends while the cold spell duration has a statistically significant decreasing trend from 1885 to 2008. As extreme temperature events would exert profound impacts on society, public health and infrastructure design in the region (Peterson, 1981; Leung et al., 2008; Guangdong Provincial Meteorological Bureau, 2007), it is important to assess how the frequency of extreme temperature events will change

[†]Corresponding author: tclee@hko.gov.hk.

during the 21st century in response to global warming.

In 2004, the Hong Kong Observatory (HKO) conducted studies on temperature projections for Hong Kong utilizing the data of global climate model projections included in IPCC's Third Assessment Report (Leung et al., 2004b). The projections were later updated in 2007 based on model data of IPCC AR4 with the effects of urbanization on local temperature also taken into account (Leung et al., 2007). In these two studies, projections of the temperature trends in Hong Kong in the 21st century were made using the monthly mean data of simulations of the global climate models together with observed temperatures in Hong Kong and southern China through statistical downscaling techniques. The projection results showed that the increasing trend of the average temperature in Hong Kong would continue in the 21st century. Since only monthly mean temperature model data were available for the 2007 study, the estimation of the number of extreme events could only rely on additional correlation relationships between seasonal (winter or summer) mean temperature and the number of extreme events. The results showed that there would be a significant decrease in the number of cold days (daily minimum temperatures ≤ 12.0 °C) and an increase in the number of very hot days (daily maximum temperature ≥ 33.0 °C) and hot nights (daily minimum temperature ≥ 28.0 °C) in Hong Kong.

This study is undertaken to extend the previous study on extreme temperature projections using daily global climate model data for IPCC AR4 and a more direct and comprehensive statistical downscaling technique. The data and extreme temperature indices used in this study are described in Section 2. The statistical downscaling method and extreme analysis approach are presented in Section 3. Results of the projection are discussed in Section 4. Section 5 contains a summary of the study.

2. Data and extreme indices

2.1 Observations

The performance of the statistical downscaling technique (see Section 3) depends strongly on the availability and the quality of large scale (predictors)

and local scale (predictands) observational data used for developing and testing of the downscaling model. In this study, daily maximum, minimum and mean temperature data recorded at the Hong Kong Observatory Headquarters (HKOHq) from 1971 to 2000 were used as the local scale observational data (predictand). For large scale predictors, 6-h (0000, 0600, 1200, and 1800 UTC) surface and upper air (at 850- and 500-hPa levels) reanalysis grid-point data (resolutions $1.9^\circ \times 1.9^\circ$ for precipitation and $2.5^\circ \times 2.5^\circ$ for the others) over southern China (20° – 30° N, 105° – 120° E) from 1971 to 2000 were retrieved from the U.S. National Centers for Environmental Protection (NCEP) for the study. NCEP data before 1971 was not used to establish the regression equations as a previous study by Yang et al. (2002) indicated that the quality of the NCEP reanalysis data over Asia prior to 1968 may be low. Unless otherwise stated, the observed temperature in Hong Kong, the temperature anomaly, the projected temperature anomaly, and the projected temperature in Hong Kong refer to the corresponding values at HKOHq in this study.

2.2 Global climate model data

2.2.1 Time-slice data

Time slices of gridded daily data projected for the periods 2046–2065 and 2081–2100 by AR4 global climate models are available from the Program for Climate Model Diagnosis and Intercomparison (PCMDI) website (http://www-pcmdi.llnl.gov/ipcc/about_ipcc.php) (Meehl and Hibbard, 2007). Among the 6 GHG emission scenarios used by IPCC AR4 in global climate simulations (from low to high GHG emissions: B1, A1T, B2, A1B, A2, and A1FI), model data for 3 out of the 6 emission scenarios, namely A2, A1B, and B1, are available from the PCMDI website. Further details of the GHG emission scenarios employed by IPCC AR4 are documented in the "Special Report on the 6 Emission Scenarios (SRES)" (Nakicenovic et al., 2000).

Twenty-two global climate models with daily projection data available are assembled in the PCMDI website. The performance of global climate models in projecting the future climate of East Asia and southern China varies widely (Xu et al., 2007; Chan et al., 2010). This is illustrated by the scatter plot (Fig. 1) of the performance of a set of AR4 models in simulating

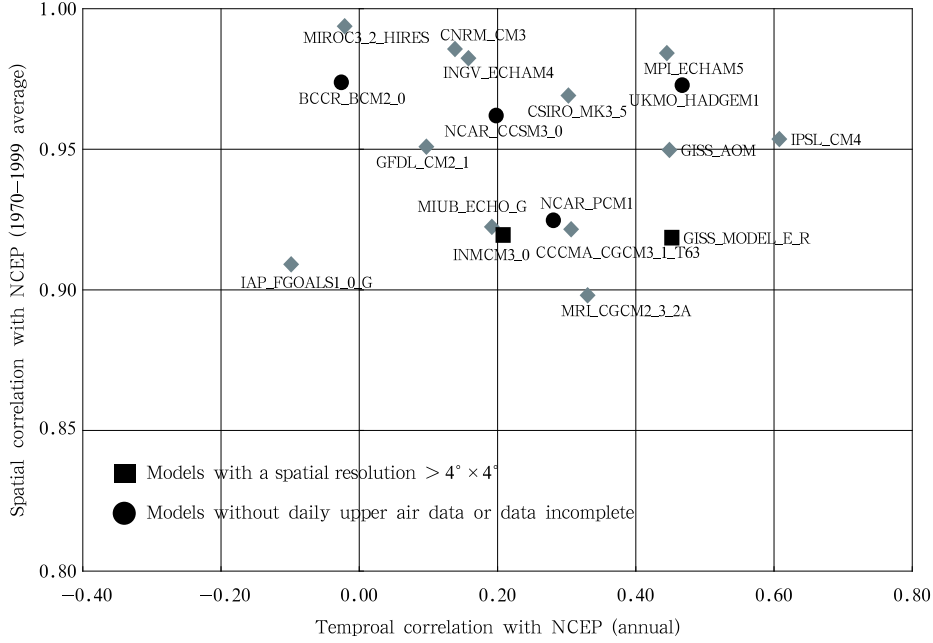


Fig. 1. Scatter plot of the performance of AR4 models.

the spatial and temporal variations of annual mean temperature in southern China for the period 1970–1999 (Chan et al., 2010). One approach to improve the performance of the ensemble mean projection is to discard less skillful models which are likely to produce large simulation errors. In this study, models satisfying the following criteria on simulation skill, spatial resolution, and data availability are used: (1) models with both daily surface and upper air data available; (2) models with spatial resolution better than $4^\circ \times 4^\circ$; (3) models with spatial correlation > 0.9 in southern China; and (4) if a climate model has more than one version, the latest model version or the version with higher spatial resolution will be used.

After a selection based on the above criteria and noting that not all three of the emission scenarios are available for each model, a total of 26 sets of model simulation data are available for this study (Table 1).

As models with daily and upper air data are required for this study, the model-scenario combination of the current study is different from that of the study in 2007 (Leung et al., 2007). To assess the effect of the change in the model-scenario combination on projection results, the multi-model scenario mean of the spatial average of the gridded model temperature

Table 1. Emission scenarios and model simulations

Model	A2	A1B	B1
CCCMA_CGCM3_1_T63	×	✓	✓
CNRM_CM3	✓	✓	✓
CSIRO_MK3_5	✓	✓	×
GFDL_CM2_1	✓	✓	✓
GISS_AOM	×	✓	✓
IAP_FGOALS1_0_G	×	✓	✓
INGV_ECHAM4	✓	✓	×
IPSL_CM4	✓	✓	×
MIROC3_2_HIRES	×	✓	✓
MIUB_ECHO_G	✓	✓	✓
MPI_ECHAM5	✓	✓	✓

✓: model simulation used; ×: data not available or incomplete.

projections over southern China (20° – 30° N, 105° – 120° E) in the 21st century for these two model-scenario combinations are compared. It is found that the differences in the annual mean temperature of southern China between these two model-scenario combinations are less than 0.1°C in the 21st century, indicating that mean temperature projections of these two model-scenario combinations for southern China are in general comparable.

Moreover, for assessing the performance of the models in reproducing the past climate, simulation data of the past climate for 1971–2000 based on the

historical GHG concentrations (20C3M scenario) of the 11 models used in this study are also retrieved from the PCMDI website for comparison (see Section 4.2).

2.2.2 Whole 21st century model data

In addition to the time slice data from PCMDI, and with a view to examining the decadal variation of extreme temperature events and possible changes in the frequency of extreme events in the 21st century, daily projection data of the GFDL_CM2_1 model (A2 and B1 scenarios) and MIROC3_2_HIRES model (A1B scenario) for the whole 21st century are respectively acquired from the Geophysical Fluid Dynamics Laboratory (GFDL) and Center for Climate System Research of the University of Tokyo/National Institute for Environmental Studies, and Frontier Research Center for Global Change of Japan Agency for Marine-Earth Science and Technology.

2.3 Extreme temperature indices

In order to rationalize and standardize the expressions for extreme weather events so that individuals, countries, and regions can calculate the related indices in the same way such that their analyses can fit together seamlessly, the Expert Team on Climate Change Detection, Monitoring and Indices (ETCCDMI) working under the joint WMO Commission for Climatology (CCL)/World Climate Research Program (WCRP) Climate Variability and Predictability (CLIVAR) project (Peterson et al., 2001; Peterson, 2005) has developed a suite of indices for the purpose. A suite of 13 extreme temperature indices to indicate the trend and significance of extreme temperature events are used in this study. They are adopted from the list of extreme indices proposed by the ETCCDMI (<http://cccma.seos.uvic.ca/ETCCDI/indices.shtml>) with appropriate modifications to suit the subtropical climate of Hong Kong. The 13 extreme temperature indices are briefly described below. Details of their definitions and deviations from those proposed by ETCCDMI, if any, are summarized in appendix for ease of reference.

CD12, SU33, and TR28 respectively represent the annual counts of cold days (daily minimum temperatures ≤ 12.0 °C), very hot days (daily maximum tem-

perature ≥ 33.0 °C), and hot nights (daily minimum temperature ≥ 28.0 °C). These three indices are modified from the indices proposed by ETCCDMI for use with reference to Hong Kong.

TX_x , TN_x , TX_n , and TN_n are the annual highest maximum temperature, highest minimum temperature, lowest maximum temperature, and lowest minimum temperature recorded every year respectively.

$TN10p$ is an index measuring the percentage of time with daily minimum temperatures lower than the 10th percentile of minimum temperatures calculated for each calendar day (with reference to the period 1971–2000) using a running 5-day window. This is a measure of the percentage of unseasonably low temperature nights (cool nights) in a year. Similarly, $TX10p$ is an index showing the percentage of unseasonably low temperature days (cool days). $TN90p$ and $TX90p$ are the indices corresponding to the percentage of unseasonably high temperature nights (warm nights) and days (warm days) in a year respectively.

The Warm Spell Duration Index (WSDI) is the annual count of days with at least 6 consecutive days with the daily maximum temperature above the 90th percentile of the maximum temperature calculated for each calendar day (with reference to the period 1971–2000) using a running 5-day window. The Cold Spell Duration Index (CSDI) is the annual count of days with at least 6 consecutive days with the daily minimum temperature below the 10th percentile of the minimum temperature calculated for each calendar day (with reference to the period 1971–2000) using a running 5-day window.

Generally speaking, $TN90p$, $TX90p$, and WSDI can be considered as “warm indices” and $TN10p$, $TX10p$, and CSDI are “cold indices”.

3. Methods

3.1 Statistical downscaling

Statistical downscaling is used to generate local scale climate projections from global climate model forecasts that are usually made at a relatively coarse spatial resolution, typically $300 \text{ km} \times 300 \text{ km}$ (e.g., Kilsby et al., 1998). It is a popular approach because it is computationally economic compared with

the alternative method of dynamical downscaling (see Fan et al., 2005), and it has a level of skill on a par with the dynamical approach (Murphy, 1999). This is also the technique used by HKO in the previous temperature projection studies in 2004 and 2007 (Leung et al., 2004b, 2007). In the present study, the daily temperature projections for southern China from global climate models are downscaled to Hong Kong. Firstly, a regression relationship between the temperature data at HKOHq and the large scale surface and upper air observations (temperature, specific humidity, and winds) over southern China is developed using past observational data. The spatial average of the NCEP reanalysis grid-point daily data (surface and upper air) bounded by 20° – 30° N, 105° – 120° E are used as the large scale predictors (see Table 3) and the HKOHq daily maximum, mean and minimum temperature with the urbanization effect removed (see Section 3.1.1) are used as local predictands. As the effect of precipitation on local temperature is likely to be confined to the nearby region, a smaller domain (21.25° – 26.25° N, 111.25° – 116.25° E) is used

for the spatial average of the precipitation predictor. The global climate model projection data for southern China is then input into the regression relationship to obtain the projections of daily temperatures for Hong Kong without the urbanization effect. Lastly, the projected temperature increase due to future urbanization effect is added to the daily temperature projections without urbanization to give the final daily temperature projections for Hong Kong in the 21st century. To reduce the systematic bias of global climate model predictors, the data are standardized prior to performing the statistical downscaling (see Section 3.1.2).

Figure 2 shows the schematic diagram of the workflow for the statistical downscaling method used. Further descriptions on the key steps are documented in Sections 3.1.1–3.1.6.

3.1.1 Removal of the urbanization effect

As pointed out by Leung et al. (2007), surface temperature observations are not used directly in NCEP reanalysis data and the data set is relatively free from the urbanization effect (Kalnay and Cai, 2003). To align with the large scale predictors,

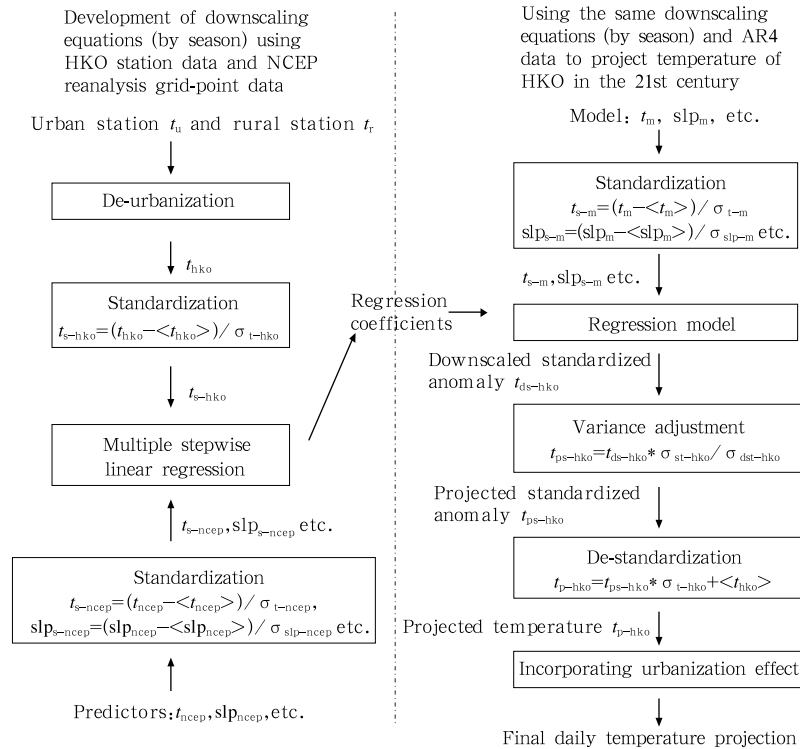


Fig. 2. Schematic diagram of the workflow for statistical downscaling.

the temperature data of HKOHq without urbanization (de-urbanized temperature) are therefore used as the predictands to set up the regression relationship for downscaling.

The magnitude of urbanization effect on temperature (T_{u-r}) is usually taken as the temperature difference between an urban station and a rural station (Karl et al., 1988; Arnfield, 2003). In this study, HKOHq is taken as the urban station. For rural station, Fong et al. (2009) recently reported that the long-term temperature observations at Macao are relatively less influenced by the urbanization effect and could be considered as a suitable rural station for urbanization studies in southern China. Moreover, the distance between HKOHq and the Macao station is about 65 km, which lies within the suggested range between rural and urban stations (30–100 km) in urban heat island studies (Karl et al., 1988). Hourly observations for Macao are available after 1952, but there were significant developments in some areas of Macao after 2000. To estimate the urbanization effect on the temperature in Hong Kong, the temperature data of Macao from 1952 to 2000 are used in this study. Theoretically, the temperature difference between an urban station (T_u) and a rural station (T_r) can be expressed as

$$T_u - T_r = T_{u-r} + c_1, \quad (1)$$

where T_{u-r} is the magnitude of urbanization effect on temperature and c_1 is a constant representing the temperature difference due to location and geographical differences.

Their derivatives with respect to time (i.e., the rate of change) can be expressed as:

$$\frac{\partial T_{u-r}}{\partial t} = \frac{\partial T_u}{\partial t} - \frac{\partial T_r}{\partial t}. \quad (2)$$

The mean values of the rate of change of T_{u-r} for maximum, mean, and minimum temperatures in four seasons during the period 1952–2000 are shown in Table 2. It can be seen that the urbanization effect on minimum temperature is more prominent with the highest magnitude in winter and spring. The mean rate of change of T_{u-r} is about 0.075 °C per decade, which in general agrees with the independent estimate

by Leung et al. (2007) using the temperature at Ta Kwu Ling, a rural site in Hong Kong, and the approach of differencing period means. As regard the maximum temperature, the negative values in summer and autumn suggest that the rate of increase in maximum temperature at HKOHq during this period could be on average slightly lower than that of Macao in these two seasons. Analysis of past trends revealed that the daily maximum temperature in Hong Kong has been rising, but at a slower rate when compared with that of the minimum temperature. Previous studies indicated that the effect of urbanization influences the daily minimum temperature more than the daily maximum temperature (Karl et al., 1988; Zhou et al., 2004). This may be due to the effect of daytime shading, which partly blocks solar radiation from reaching the ground in urban areas. In addition, the higher heat capacity and conductivity of urban areas may also be another cause (Bornstein, 1968; Oke, 1982). Another possible factor hindering the increase in the maximum temperature is the increase in the cloud amount and decrease in solar radiation. One potential cause for the increase in cloud amount over Hong Kong could be the likely increase in the concentration of condensation nuclei in the air that favors the formation of clouds, which is known to be associated with urbanization and human activity in the region (Leung et al., 2004a). Both the increase in the concentration of suspended particulates and the increase in cloud amount would reduce the amount of solar radiation reaching the surface, resulting in lower temperature during the day (Wild et al., 2007; Zhang et al., 2009). As a result, the diurnal temperature range (DTR) decreases as the daily minimum rises on average faster than the daily maximum temperature (see Fig. 3). The decrease is found more pronounced in the 1980s and 1990s, likely due to the combined effect of rapid urbanization and an increase in cloud amount after the 1970s.

The de-urbanized temperature in Hong Kong is then taken as the HKOHq temperature minus the corresponding urbanization contribution.

3.1.2 Data standardization

To reduce systematic biases in the mean and variance of global climate model predictors, the data are standardized for each season by subtracting the mean and then dividing by the standard deviation of the

Table 2. Seasonal and annual rate of change of urban heat island intensity (T_{u-r}) for maximum, mean, and minimum temperatures in Hong Kong during 1952–2000

	Spring ($^{\circ}\text{C}/\text{decade}$)	Summer ($^{\circ}\text{C}/\text{decade}$)	Autumn ($^{\circ}\text{C}/\text{decade}$)	Winter ($^{\circ}\text{C}/\text{decade}$)	Annual ($^{\circ}\text{C}/\text{decade}$)
Maximum	0.018	-0.073	-0.013	0.031	-0.008
Mean	0.105	0.027	0.042	0.115	0.075
Minimum	0.166	0.115	0.133	0.201	0.154

Note: HKOHq and Macao are taken as the urban station and rural station respectively.

predictor (same for predictand) for a reference period prior to performing the statistical downscaling (Schubert, 1998; Wilby et al., 2004; Cheng et al., 2008). In this study, the period 1980–1999 (the period chosen by IPCC AR4 as the reference period for the evaluation of projections into the 21st century) is taken as the reference period for preparing the standardized anomalies. Mathematically, the standardized anomaly for a variable X is

$$X_{\text{std}} = \frac{X - \langle X \rangle}{\sigma}, \quad (3)$$

where $\langle X \rangle$ is the mean and σ is the standard deviation of X over the reference period (1980–1999).

3.1.3 Setting up downscaling equations

The stepwise multiple linear regression (Wilks, 2006; Crawley, 2008) is employed in this study to develop the statistical downscaling equations. For each of the three predictands (daily maximum, mean, and minimum temperature), a multiple linear regression relationship between the standardized predictand (de-urbanized temperature data at HKOHq) and a set of 15 standardized NCEP re-analysed spatially averaged

daily surface and upper air variables over southern China is established for each season using historical data from 1971 to 2000. Here, spring refers to the period from March to May, summer from June to August, autumn from September to November, and winter from December to February. Table 3 listed the predictors and predictands used in this study. The choice of the predictors has also been constrained by data availability from the PCMDI. Besides surface variables, large scale circulation predictors with data available from PCMDI at two standard upper air levels (850 and 500 hPa) are also used. Table 4 summarizes the predictors and coefficients of the regression equations used in this study.

3.1.4 Downscaling of daily model data

Standardized anomalies of global climate model data over southern China are fed into the corresponding multiple linear regression equations developed in Section 3.1.3 to produce the downscaled standardized anomaly of temperature element (say daily maximum temperature) for Hong Kong. In order to adjust for the difference of variance between the observed and

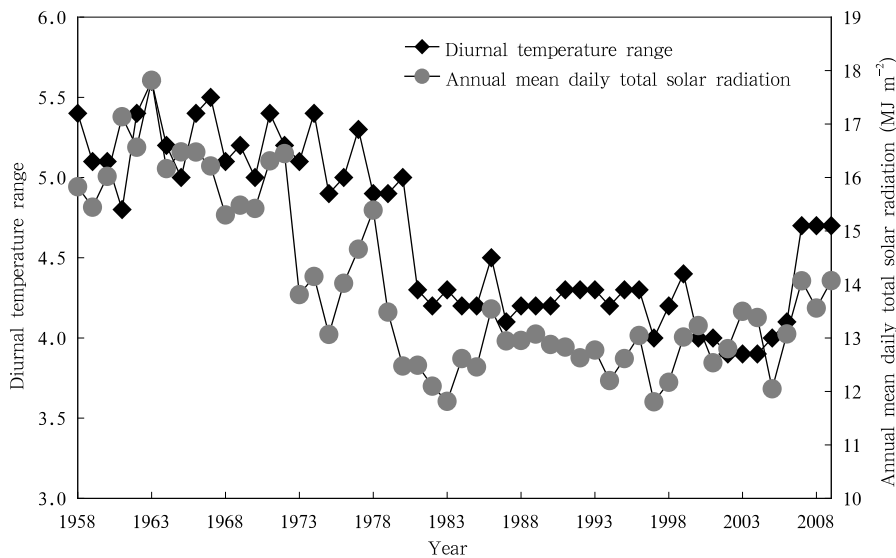
**Fig. 3.** Annual mean daily total solar radiation and diurnal temperature range.

Table 3. Predictands and predictors used in this study

Predictands	Predictors
Daily mean temperature at HKOHq (Mean)	Surface mean temperature (Tmean)
Daily maximum temperature at HKOHq (Max)	Surface maximum temperature (Tmax)
Daily minimum temperature at HKOHq (Min)	Surface minimum temperature (Tmin)
	Sea level pressure (Slp)
	Surface eastward component of wind (U)
	Surface northward component of wind (V)
	Precipitation (Pr)
	850-hPa temperature (T850)
	850-hPa specific humidity (Sh850)
	850-hPa eastward component of wind (U850)
	850-hPa northward component of wind (V850)
	500-hPa temperature (T500)
	500-hPa specific humidity (Sh500)
	500-hPa eastward component of wind (U500)
	500-hPa northward component of wind (V500)

Table 4. Predictors and standardized coefficients of the regression equations used for each of the three predictands (daily maximum, mean, and minimum temperature) in four seasons

Predictors	Spring			Summer			Autumn			Winter		
	Max	Mean	Min									
Tmax	×	×	×	×	×	×	-0.56	×	×	-0.34	×	×
Tmean	0.64	0.74	0.57	0.28	0.31	-0.12	1.62	1.11	0.75	1.14	0.97	0.60
Tmin	×	×	0.30	×	×	0.36	×	×	0.43	×	×	0.36
Slp	0.07	0.05	0.05	0.03	0.03	0.05	×	0.07	0.10	-0.06	×	0.05
U	0.34	0.31	0.20	0.13	0.20	0.17	0.02	0.03	-0.03	0.05	0.04	×
V	-0.21	-0.38	-0.45	-0.42	-0.56	-0.37	-0.35	-0.47	-0.45	-0.49	-0.73	-0.69
Pr	×	0.03	0.04	-0.29	-0.22	-0.23	-0.12	-0.07	-0.06	-0.14	-0.09	-0.08
T850	0.24	0.21	0.15	0.33	0.38	0.36	0.09	×	×	0.37	0.27	0.23
Sh850	-0.11	-0.06	-0.08	0.04	0.10	0.12	-0.10	0.11	0.15	-0.18	-0.07	×
U850	-0.30	-0.21	-0.06	×	×	-0.12	0.12	0.12	0.16	-0.06	0.05	0.12
V850	0.13	0.24	0.25	×	0.15	0.10	×	0.15	0.14	×	0.20	0.25
T500	0.13	0.11	0.10	×	0.03	0.09	×	×	×	0.04	0.03	0.02
Sh500	-0.06	×	0.02	-0.17	-0.16	-0.20	-0.04	0.02	×	-0.10	-0.05	-0.03
U500	-0.05	×	-0.03	0.18	0.29	0.37	-0.08	×	0.06	×	×	×
V500	0.12	0.07	0.05	0.18	0.20	0.15	-0.05	-0.06	-0.04	0.10	0.04	×

×: not included as predictor in the regression equations.

downscaled data (e.g., Karl et al., 1990; Huth, 1999), the downscaled standardized temperature anomaly for Hong Kong (t_{ds-hko}) is multiplied by a factor ($\sigma_{st-hko}/\sigma_{dst-hko}$) to give the projected standardized temperature anomaly for Hong Kong (t_{ps-hko}), where σ_{st-hko} and $\sigma_{dst-hko}$ are the standard deviation of the standardized temperature anomaly in 1980–1999 and the standard deviation of the downscaled standardized temperature anomaly in 1980–1999 respectively (see Eq. (4)).

$$t_{ps-hko} = t_{ds-hko} * \sigma_{st-hko} / \sigma_{dst-hko}. \quad (4)$$

The projected standardized temperature anomaly

is then de-standardized (see Eq. (5)) to give the projected temperature in Hong Kong (t_{p-hko}) without the urbanization effect.

$$t_{p-hko} = t_{ps-hko} * \sigma_{t-hko} + \langle t_{hko} \rangle, \quad (5)$$

where $\langle t_{hko} \rangle$ and σ_{t-hko} are the mean and standard deviation of HKO temperature in 1980–1999 respectively.

3.1.5 Projection of the urbanization effect

Empirically, some researchers (Oke, 1973; Torok et al., 2001) suggested that the urbanization effect on temperature may be directly proportional to the logarithm of population. With this assumption, the

relationship between the urbanization effect on temperature (T_{u-r}) and the logarithm of population ($\lg P$) can be expressed as

$$T_{u-r} = a \lg P + c_2, \quad (6)$$

where a is the correlation coefficient and c_2 is a constant. Therefore, the rate of change of T_{u-r} can be related to the rate of change in the logarithm of population as

$$\frac{\partial T_{u-r}}{\partial t} = a \frac{\partial \lg P}{\partial t}. \quad (7)$$

As Fig. 4 shows, the rate of change of $\lg P$ in Hong Kong is expected to slow down in the future (Census and Statistics Department, 2007). A quantitative estimate suggests that the average increasing rate of $\lg P$ over the period 2009–2036 will be about 1/4 of that of 1885–2008. As such, a future urbanization scenario in which the rate of temperature change due to the urbanization effect in the 21st century is 1/4 of that of 1885–2008 is adopted in this study.

3.1.6 Temperature projections incorporating the urbanization effect

The urbanization effect assumed in Section 3.1.5 is added to the daily temperature projections without urbanization effect (t_{p-hko}) in Section 3.1.4 to give the final daily temperature projections in Hong Kong in the 21st century.

3.2 Time-dependent return period analysis

The long-term trends of the variation of the return period of extreme temperatures in Hong Kong

in the 21st century is studied by applying the time-dependent Generalized Extreme Value (GEV) distribution technique (Coles, 2001) to the projected daily maximum and minimum temperatures in Hong Kong. The data are downscaled from the GFDL_CM2_1 model (A2 and B1 scenarios) and MIROC3_2_HIRES model (A1B scenario) where daily data for the whole 21st century are available. As the principles and analysis method of the time-dependent GEV distribution technique have been well documented in other reference publications (Kharin and Zwiers, 2005; Wong and Mok, 2009), they are not repeated here.

4. Results and discussion

4.1 Validation of the downscaling equations

The correlation coefficients (R) for the 12 downscaling equations (for maximum, minimum, and mean temperatures for each of the 4 seasons) developed based on the method described in Section 3 range from 0.67 to 0.95. Higher correlations are found in autumn and spring while the correlation is relatively lower in summer.

The cross validation method is employed to evaluate the goodness of fit of the downscaling equations in predicting the daily temperatures. The cross validation consists of omitting about 5% of data in turn when setting up the regression equation. The regression equation developed based on the remaining

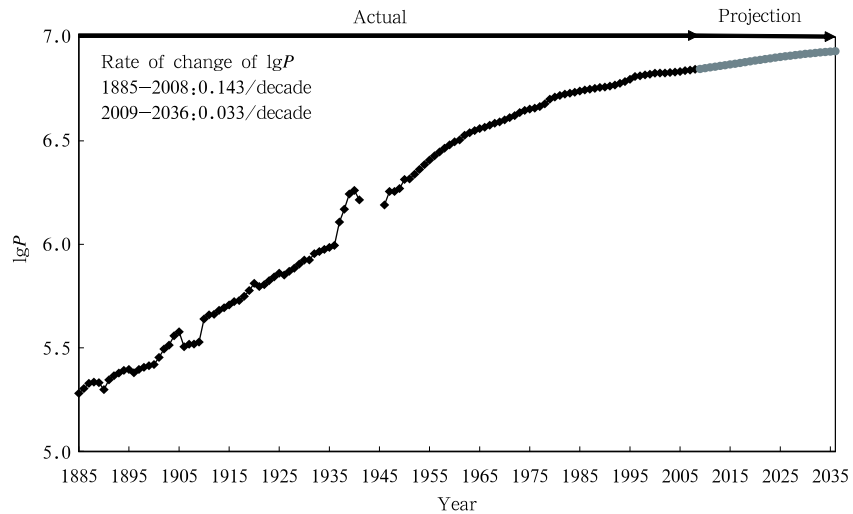


Fig. 4. Time series of the logarithm of population ($\lg P$) in Hong Kong (1885–2036).

data is applied to predicting the omitted data (Wilks, 2006; Crawley, 2008). The root mean square (rms) errors of the cross validation for the 12 equations are all below 1.5 °C, except for the maximum temperature in spring (2.1 °C) and winter (1.7 °C).

4.2 Evaluation of model performance in simulating the past climate

In order to verify the performance of the global climate models in simulating the past extreme temperature events, the ensemble means of the annual numbers of very hot days, hot nights and cold days estimated from the downscaled model data for 1971–2000 (under the 20C3M scenario) are compared with the actual figures for Hong Kong (Table 5). Although the skill of each model in simulating the three indices varies, the multi-model ensemble mean values are in general comparable to the actual observations. The errors for very hot days, hot nights and cold days are respectively 3.6, 1.0, and –0.6 days, which are well within one standard deviation of the corresponding distribution of the observed extreme events in 1971–2000 (i.e., 5.6 days, 8.7 nights, and 7.8 days, respectively). More detailed analysis of the data at a 5-yr

interval (Fig. 5) shows that the climate models in general have an acceptable skill in simulating the numbers of hot nights and cold days. However, the number of very hot days reproduced by the models is on the high side when compared with the actual observation, especially in the 1980s and 1990s. The models have simulated a rising trend in the number of very hot days during this period, while there is a slight decrease in the actual observation.

Table 5. Average annual numbers of very hot days, hot nights and cold days observed in Hong Kong during 1971–2000 and the corresponding estimations obtained from the downscaled data under the 20C3M scenario

Model/Actual	Very hot days	Hot nights	Cold days
Model ensemble mean	13.4	14.1	18.0
Actual	9.8	13.1	18.6
Standard deviation of the actual observation during 1971–2000	5.6	8.7	7.8

This could be due to the fact that the models are less skillful in simulating the high temperature extremes (Sterl et al., 2008) and the statistical downscaling technique could not completely remove the possible model bias on the maximum temperature distribution.

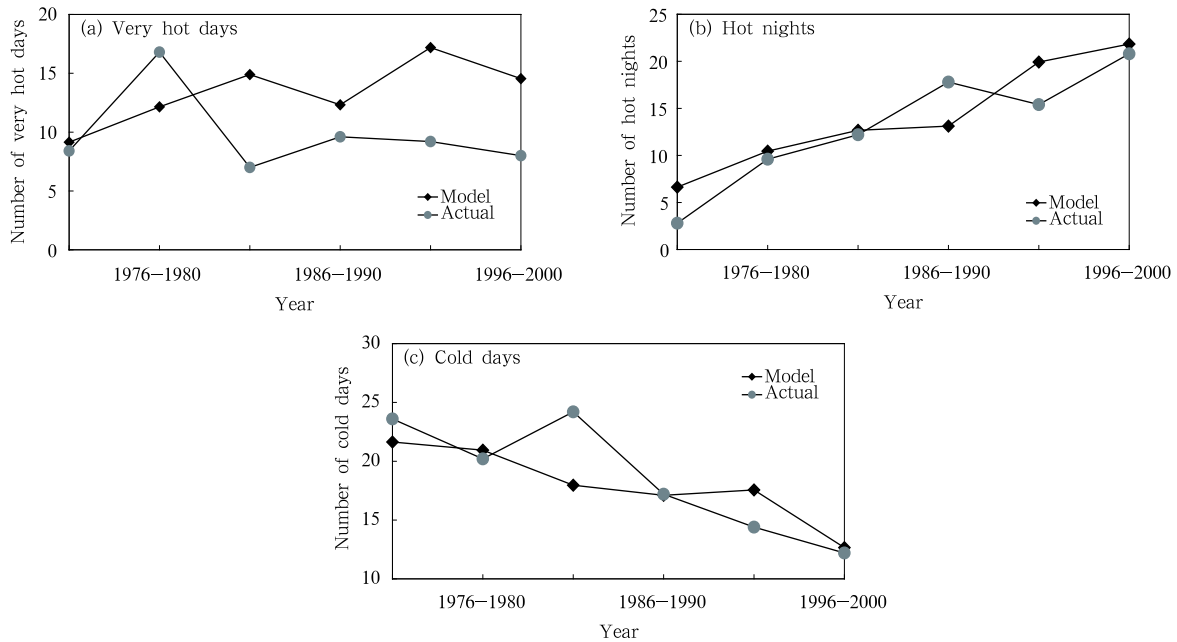


Fig. 5. The 5-yr average numbers of (a) very hot days, (b) hot nights, and (c) cold days observed in Hong Kong during 1971–2000 and the corresponding model ensemble mean estimation obtained from the downscaled data of 11 models under the 20C3M scenario.

Moreover, localized changes in urbanization and solar radiation in the last few decades could also contribute to the discrepancy between the simulated and observed number of very hot days. As mentioned in Section 3.2.1, Hong Kong has undergone rapid development since the 1970s and the solar radiation in Hong Kong was in a low phase during the 1980s and 1990s. The lower solar radiation period during the 1980s and 1990s coupled with the urbanization effect could have affected the daily maximum temperature, resulting in relatively lower number of very hot days. The models probably could not adequately capture these localized effects on the daily maximum temperature and predict a higher number of very hot days during this period. In fact, with the rebound of solar radiation and the slowing down of urbanization in the 2000s, the average number of very hot days for the 5-yr period 2005–2009 increases to about 17 days.

As regard hot nights and cold days, since the night time minimum temperature is mainly affected by thermal radiative exchanges (e.g., radiative cooling), the climate models driven by the 20C3M scenario display a reasonable skill in depicting the enhanced greenhouse effect on the trend of these events in the past.

4.3 Projection results

4.3.1 Maximum, minimum, and mean temperatures

Table 6 summarizes respectively the changes in the annual mean maximum, mean, and minimum temperatures in Hong Kong (multi-model scenario ensemble mean relative to the average of 1980–1999) for the decades 2050–2059 and 2090–2099.

For the three emission scenarios (B1, A1B, and

Table 6. Projected changes in the annual mean maximum, mean, and minimum temperatures in Hong Kong (relative to the average of 1980–1999) for the decades 2050–2059 and 2090–2099

Parameter		2050–2059	2090–2099
Maximum temperature	Ensemble upper limit	2.8	4.9
	Ensemble mean	2.0	3.3
	Ensemble lower limit	1.2	1.5
Mean temperature	Ensemble upper limit	3.0	5.0
	Ensemble mean	2.1	3.5
	Ensemble lower limit	1.3	1.7
Minimum temperature	Ensemble upper limit	3.5	5.6
	Ensemble mean	2.4	4.0
	Ensemble lower limit	1.6	2.2

A2), all models predict positive anomalies for the maximum, mean, and minimum temperature in the decades 2050–2059 and 2090–2099. The multi-model scenario ensemble average suggests that, relative to the average of 1980–1999, the annual mean maximum, mean, and minimum temperature in the decade 2090–2099 would increase by 3.3, 3.5, and 4.0 °C respectively. The 3.5 °C increase in the mean temperature is within the best estimate range of the projected global average rise (1.8–4 °C) given in the IPCC AR4.

Figure 6 shows the projected annual mean temperature anomaly in Hong Kong for the whole 21st century period given by the GFDL_CM2_1 model (A2 and B1 scenarios) and MIROC3_2_HIRES model (A1B scenario) together with the spread of the projection of all the model-scenario combinations for the decades 2050–2059 and 2090–2099. The increasing trend of the annual mean temperature in Hong Kong will continue in the 21st century. The B1 scenario of the GFDL_CM2_1 model has a temperature projection near the lower bound of the spread while the A1B scenario of the MIROC3_2_HIRES model has a projection close to the upper bound of the spread. A similar increasing trend is also found in the annual mean maximum and minimum temperature projections (figures omitted).

4.3.2 Very hot days (SU33), hot nights (TR28), and cold days (CD12)

The projected annual numbers of very hot days and hot nights in Hong Kong for different emission scenarios are given in Tables 7 and 8 respectively. Figures 7 and 8 also show the projected annual mean number of very hot days and hot nights in Hong Kong for the whole 21st century period given by the GFDL_CM2_1 model (A2 and B1 scenarios) and MIROC3_2_HIRES model (A1B scenario) together with the spread of the projection of all the model-scenario combinations for the decades 2050–2059 and 2090–2099. It can be seen that the numbers of very hot days and hot nights increase significantly in the 21st century with the multi-model scenario ensemble mean reaching about 89 days per year and 137 nights per year respectively in the decade 2090–2099. Other

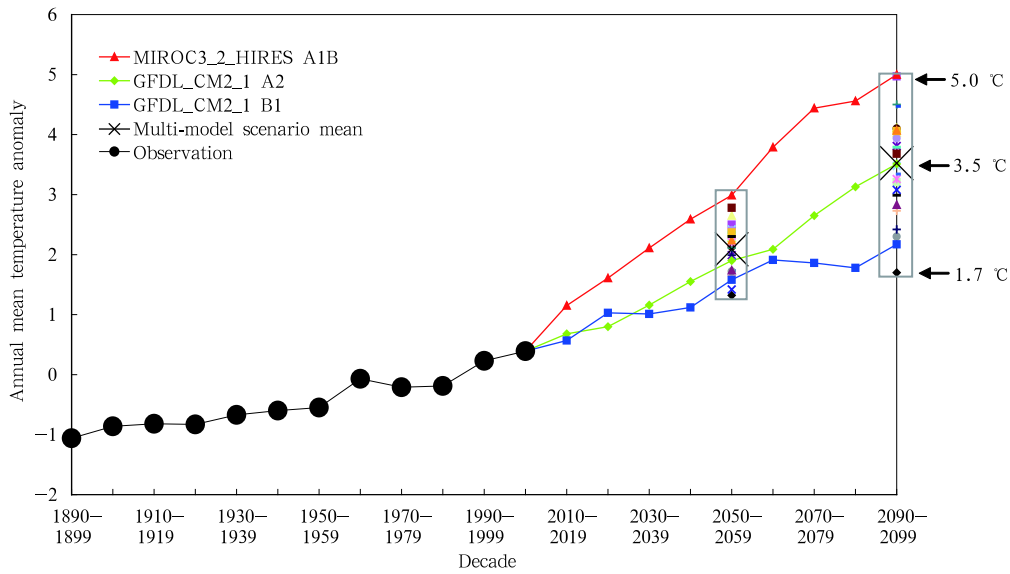


Fig. 6. Projected annual mean temperature anomaly in Hong Kong for the whole 21st century period given by the GFDL_CM2_1 model (A2 and B1 scenarios) and MIROC3_2_HIRES model (A1B scenario) together with the spread of the projection of all the model-scenario combinations for the decades 2050–2059 and 2090–2099. The annual mean temperature in Hong Kong is expected to increase from 23.1 °C in 1980–1999 to 26.6 °C (black cross) in 2090–2099.

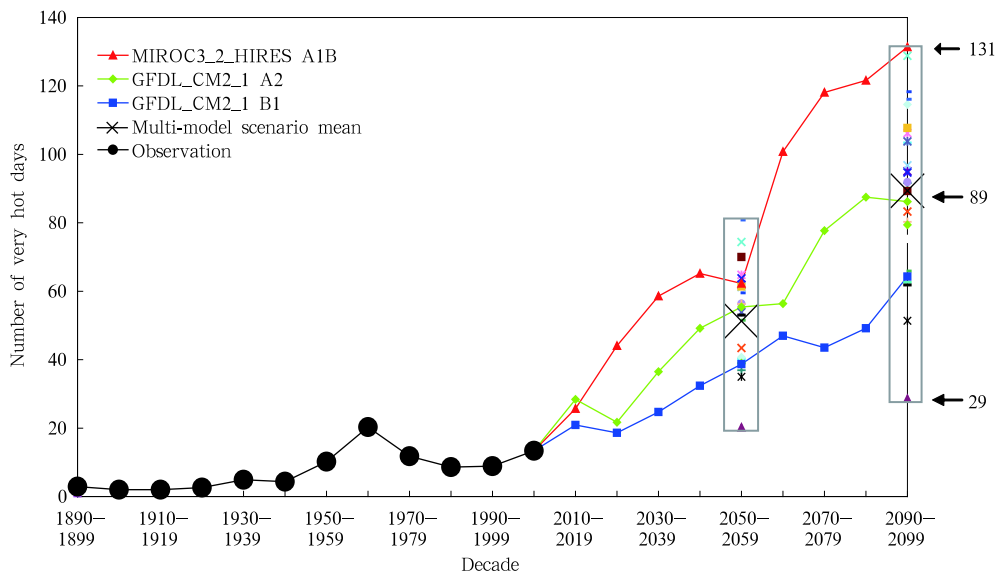


Fig. 7. Projected annual mean number of very hot days in Hong Kong for the whole 21st century period given by the GFDL_CM2_1 model (A2 and B1 scenarios) and MIROC3_2_HIRES model (A1B scenario) together with the spread of the projection of all the model-scenario combinations for the decades 2050–2059 and 2090–2099. The average annual number of very hot days is expected to increase from the average of 9 days in 1980–1999 to 89 days (black cross) in 2090–2099.

model simulation studies in Japan and Canada also suggest that the number of extreme high temperature events would considerably increase by several folds to-

wards the end of the 21st century (Pancura and Lines, 2005; IPCC, 2007b; Cheng et al., 2008).

The projected annual number of cold days in

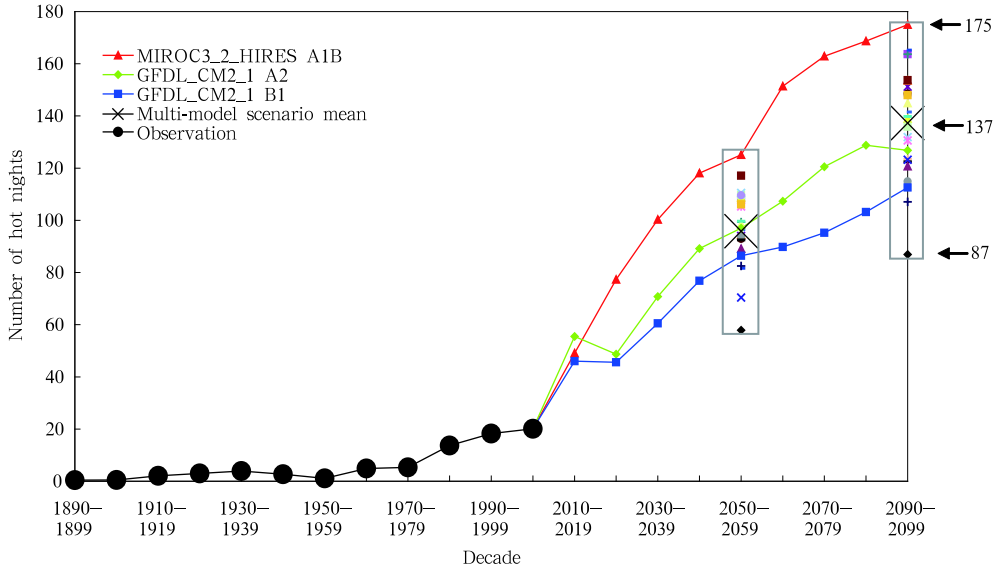


Fig. 8. As in Fig. 7, but for hot nights. The average annual number of hot nights is expected to increase from the average of 16 nights in 1980–1999 to 137 nights (black cross) in 2090–2099.

Table 7. Projected annual number of very hot days in Hong Kong for different emission scenarios

Parameter	2050–2059	2090–2099
Ensemble mean for B1 (M_{B1})	44.9	66.4
Ensemble mean for A1B (M_{A1B})	56.2	96.3
Ensemble mean for A2 (M_{A2})	52.7	105.4
Ensemble upper limit	80.8	131.4
Ensemble mean for 3 scenarios (mean of M_{B1} , M_{A1B} , and M_{A2})	51.3	89.4
Ensemble lower limit	20.2	28.6

The average annual number of very hot days in 1980–1999 is 9 days.

Table 8. Projected annual number of hot nights in Hong Kong for different emission scenarios

Parameter	2050–2059	2090–2099
Ensemble mean for B1 (M_{B1})	86.2	117.7
Ensemble mean for A1B (M_{A1B})	103.9	143.0
Ensemble mean for A2 (M_{A2})	97.4	151.1
Ensemble upper limit	125.1	175.0
Ensemble mean for 3 scenarios (mean of M_{B1} , M_{A1B} , and M_{A2})	95.9	137.3
Ensemble lower limit	57.9	86.9

The average annual number of hot nights in 1980–1999 is 16 nights.

Hong Kong for different emission scenarios is given in Table 9. Figure 9 also shows the projected annual mean number of cold days in Hong Kong for the whole 21st century period given by the GFDL_CM2_1 model (A2 and B1 scenarios) and MIROC3_2_HIRES model (A1B scenario) together with the spread of the projection of all the model-scenario combinations for the decades 2050–2059 and 2090–2099. It can be seen

that the number of cold days decreases significantly in the 21st century with the multi-model scenario ensemble mean dropping to about 1 day per year in the decade 2090–2099. Among the 26 model-scenario combinations, 17 of them (65%) predict that the average annual number of cold days would drop to below 1 day in the decade 2090–2099. Eight percent of the model-scenarios even indicate that the average number of cold days would become less than 1 day in the decade 2050–2059.

We now take another approach to study the frequency of extreme temperature events. It is hypothetically assumed that the change in the distribution of temperature in Hong Kong from 1971–2000 to 2090–2099 only involves a simple shift in the mean but no

Table 9. Projected annual number of cold days in Hong Kong for different emission scenarios

Parameter	2050–2059	2090–2099
Ensemble mean for B1 (M_{B1})	4.3	2.4
Ensemble mean for A1B (M_{A1B})	3.0	1.0
Ensemble mean for A2 (M_{A2})	3.4	0.5
Ensemble upper limit	7.7	5.3
Ensemble mean for 3 scenarios (mean of M_{B1} , M_{A1B} , and M_{A2})	3.6	1.3
Ensemble lower limit	0.8	0.0
Percentage of the model-scenario combination with annual number of cold days < 1	8%	65%

The average annual number of cold days in 1980–1999 is 17 days.

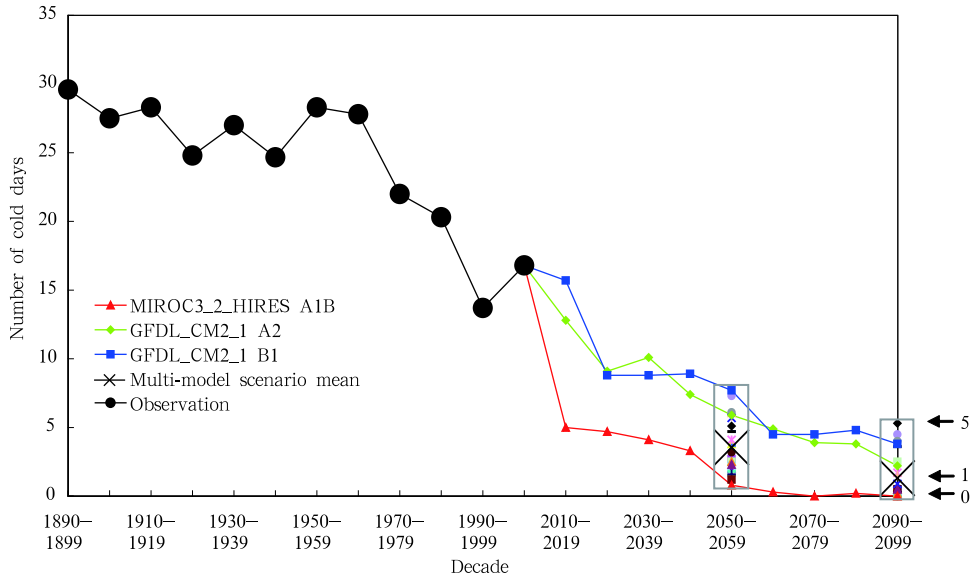


Fig. 9. As in Fig. 7, but for cold days. The average annual number of cold days will drop from the average of 17 days in 1980–1999 to 1 day (black cross) in 2090–2099.

change in the variance (as illustrated in Fig. 10, modified based on Houghton (2009)), and the number of extreme high and low temperature events in the new climate are calculated. Table 10 summarizes the numbers of very hot days, hot nights, and cold days in the decade of 2090–2099 with increases of 1 to 5 °C in the mean but with the same shape of distribution of the set of 1971–2000 temperatures. If the mean of the maximum temperature distribution of 1971–2000 increases, say by 3–4 °C, the number of very hot days and hot nights could increase to 100–126 days and 115–146 nights respectively in 2090–2099. Similarly, a 4 °C increase in the mean minimum temperature

Table 10. Annual numbers of very hot days, hot nights, and cold days in the decade 2090–2099 as estimated from 1 to 5 °C increase in the mean of the 1971–2000 temperature distribution in Hong Kong

Temperature	Very hot days	Hot nights	Cold days
T+1	40	43	12
T+2	72	79	8
T+3	100	115	5
T+4	126	146	3
T+5	152	171	2

will bring the number of cold days down to about 3 days in 2090–2099. The results of the current study match with these orders of magnitude reasonably well.

4.3.3 Other extreme indices

Table 11 summarizes the projections (multi-model scenario ensemble mean) of the other 10 extreme indices for the decades 2050–2059 and 2090–2099 as well as the average of the observed values in 1980–1999.

Similar to the results obtained in Sections 4.3.1 and 4.3.2, TX_x , TN_x , TX_n , TN_n , $TN90p$, $TX90p$, and WSDI increase significantly in the 21st century while all the “cold indices” ($TN10p$, $TX10p$, and CSDI) decrease considerably. Moreover, all of the model-scenario combinations forecast that the CSDI will drop to zero in the decade 2090–2099.

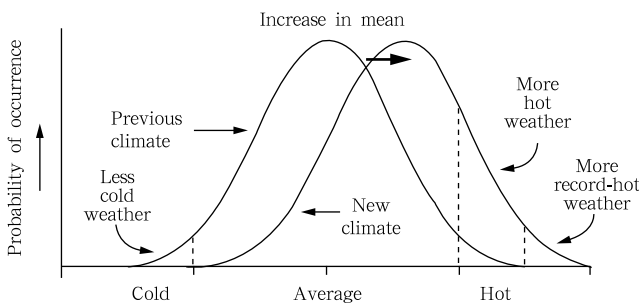


Fig. 10. A shift in the mean of the temperature distribution with the standard deviation remaining constant (modified based on Houghton (2009)).

Table 11. Projections (multi-model scenario ensemble mean) of the other 10 extreme indices in Hong Kong for the decades 2050–2059 and 2090–2099 as well as the average of the observed values in 1980–1999

Extreme indices	1980–1999	2050–2059	2090–2099
TX x (°C)	34.3	36.6	38.0
TN x (°C)	29.0	32.0	33.8
TX n (°C)	10.8	14.4	16.1
TN n (°C)	7.4	10.9	12.6
TN10 p (%)	9.4	1.0	0.3
TX10 p (%)	10.8	2.1	0.8
TN90 p (%)	11.6	53.4	74.2
TX90 p (%)	8.9	35.5	57.6
WSDI (day)	2.7	73.9	156.5
CSDI (day)	1.8	0.1	0.0

4.3.4 Return period analysis

Using the actual observations for 2000–2008 and the projected annual maximum and minimum temperatures for the rest of the 21st century downscaled from the data of the GFDL_CM2_1 model (A2 and B1 scenarios) and MIROC3_2_HIRES model (A1B scenario), the time dependent GEV technique is applied to analyzing the return periods for temperatures ≤ 7 °C and ≥ 36 °C in Hong Kong by 2050. The 7 °C and 36 °C are used as references since 7 °C is considered as “very cold” in Hong Kong (HKO, 2009) and the highest maximum temperature recorded at HKOHq from 1885 to 2009 is 36.1 °C. The results together with those obtained using the observed data over the period 1885–2008 are summarized in Table 12. It can be seen that, for the GFDL_CM2_1 model (A2 and B1 scenarios), the return period for temperature ≤ 7 °C will increase significantly from 2 yr in 2000 to around 22–30 yr in 2050. For the MIROC3_2_HIRES model (A1B scenario), which has a relatively higher temperature projection, temperature ≤ 7 °C will not occur during 2009–2099 with a return period > 100 yr in 2050. On the other hand, the return period for temperature ≥ 36 °C will decrease from 38 yr in 2000 to around 1–2 yr after 2050. This suggests that, in the 21st century, extremely high temperature events would become more frequent and common, but extremely low temperature events would become increasingly rare.

4.4 Uncertainties

Although the projected changes in extreme events reported by the IPCC AR4 in general match with the

Table 12. Projected return periods for minimum temperature ≤ 7 °C and maximum temperature ≥ 36 °C in Hong Kong in 2050 for the GFDL_CM2_1 model (A2 and B1 scenarios) and MIROC3_2_HIRES model (A1B scenario) using the time dependent GEV approach with actual observations for 2000–2008 and model projections for 2009–2099. The return periods for minimum temperature ≤ 7 °C and maximum temperature ≥ 36 °C in 2000 as computed based on the observations from 1885 to 2008 are 2 and 38 yr respectively

Model	Return period (yr)	
	for minimum temperature ≤ 7 °C in 2050	for maximum temperature ≥ 36 °C in 2050
GFDL_CM2_1 (A2 scenario)	30	2
GFDL_CM2_1 (B1 scenario)	22	2
MIROC3_2_HIRES (A1B scenario)	> 100	1

observed changes in the past century, it is important to note that large uncertainties and gaps in our knowledge of climate change and extremes remain (WMO, 2009). The projections of changes in extremes are subject to uncertainties in the forcing emission scenarios, the downscaling methodology, the future urbanization effect, the choice of models, model skills as well as the response of models to different emission scenarios and aerosol effects (STARDEX, 2005; Knutti, 2008).

5. Conclusions

An extreme weather event is an infrequent event. It may not be possible to attribute an individual extreme event to climate change alone. However, a relatively small shift in the mean and the shape of the temperature distribution due to the increase in the anthropogenic greenhouse gas concentration can result in substantial changes in the frequency of extreme temperature events (Meehl et al., 2000; Meehl and Tebaldi, 2004; Kharin and Zwiers, 2005). As such, one can expect that the likelihood of an extreme high (low) temperature event will increase (decrease) in a warmer climate (Mitchell et al., 2006) in the 21st century.

Daily projection data instead of monthly mean

data are used in this study. Projections of extreme temperatures in Hong Kong for the 21st century are made by statistically downscaling 26 sets of the daily global climate model projections (11 models) of the IPCC AR4 for the three available greenhouse gas emission scenarios, namely A2, A1B, and B1. The higher temporal resolution daily projections eliminate the need for additional correlation relationships between seasonal mean temperature and the number of extreme events and should thus better depict the climate of extreme temperature events than using the monthly mean projections. The downscaling method is validated using the cross validation method. By using the 20C3M simulation data, the multi-model ensemble mean of the downscaled global climate model outputs is also verified to have an acceptable skill in reproducing past extreme temperature events during 1971–2000. The verification also suggests that the models in general are more skillful in simulating the past climate of hot nights and cold days than that of very hot days. The model simulated number of very hot days, though with a difference less than one standard deviation of the corresponding distribution, is still on the high side when compared with the actual observations. This could be due to the limitation of the model skill in simulating the extreme high temperatures and the deficiency of the statistical downscaling method in removing all the model biases. Also, the models may not be able to capture the localized effects of urbanization and changes in solar radiation on the daily maximum temperature during the 1980s and 1990s, resulting in less satisfactory simulations of the number of very hot days.

All the model-emission scenario projections suggest that the significant trends in temperature extremes that have been observed during the 20th century are expected to continue into the 21st century with a substantial increase in hot nights and very hot days and a decrease in cold days. Nevertheless, there is a large divergence in the projection for the number of extreme temperature events simulated by different model-emission scenario combinations. This, to a certain extent, reflects that there are still large uncertainties in the model simulation of the future

climate, depending very much on the future forcing emission scenarios, local urbanization effect as well as the models' characteristics/performance. Moreover, as pointed out by Reifen and Toumi (2009), a model that performs better in the verification period may not outperform other models and the multi-model ensemble mean in future projections. This is because the climate feedback strength and forcing are not stationary during the projection period and each model may respond differently to the feedback strength, favoring no particular model consistently. The generally accepted approach, the one adopted in this study for Hong Kong in the 21st century, is to use the multi model-scenario ensemble mean to depict the plausible trend in extreme temperature events (STARDEX, 2005; Kiktev et al., 2007; IPCC, 2007a; Knutti, 2008; Fowler and Ekström, 2009).

Based on the multi-model scenario ensemble mean, the average annual numbers of very hot days and hot nights in Hong Kong are expected to increase significantly from 9 days and 16 nights in 1980–1999 to 89 days and 137 nights respectively in 2090–2099. On the other hand, the average annual number of cold days will drop from 17 days in 1980–1999 to about 1 day in 2090–2099. About 65 percent of the model-scenario combinations indicate that there will be on average less than one cold day in 2090–99. Return period analysis of the projections from the GFDL_CM2_1 model (A2 and B1 scenarios) and MIROC3_2_HIRES model (A1B scenario) also suggests that the return period of a minimum temperature of 7 °C is expected to increase substantially from 2 yr in 2000 to over 22 yr in 2050 while the return period of a maximum temperature of 36 °C will dramatically decrease from 38 yr in 2000 to around 1–2 yr in 2050.

Acknowledgments. The authors acknowledge the IPCC AR4 modeling groups, the PCMDI and WCRP's Working Group on Coupled Modelling (WGCM) for their efforts in making available the WCRP CMIP3 multi-model dataset. Support of this dataset is provided by the Office of Science, U.S. Department of Energy. The authors are also very grateful to the GFDL and the JAMSTEC for providing the

whole 21st century daily global climate model data for the study. In particular, we would like to thank Prof. Lau Ngar-cheung of GFDL and Prof. Masahide Kimoto of the University of Tokyo for their kind assistance. The provision of observational data of Macao by the Macao Meteorological and Geophysical Bureau

is appreciated. We are also thankful to colleagues of the Hong Kong Observatory, Dr B. Y. Lee, Ms Hilda Lam, and Mr. H. Y. Mok for their useful comments on the manuscript, and to Mr. W. C. Chan and Mr. H. S. Chan for their assistance in data extraction and compilation.

APPENDIX

Definitinons of the extreme temperature indices used in this study

Extreme indices	Definition	Modifications to the ETCCDMI (if any)	Unit
CD12 (Cold days)	Annual number of days with minimum temperature ≤ 12 °C	Specific index for Hong Kong	Day
SU33 (Very Hot days)	Annual number of days with maximum temperature ≥ 33 °C	Threshold changed from 25 to 33 °C	Day
TR28 (Hot nights)	Annual number of days with minimum temperature ≥ 28 °C	Threshold changed from 20 to 28 °C	Day
TX x	Annual highest maximum temperature		°C
TN x	Annual highest minimum temperature		°C
TX n	Annual lowest maximum temperature		°C
TN n	Annual lowest minimum temperature		°C
TN10 p (Cool nights)	Percentage of days when daily minimum temperature <10th percentile: Let TN $_{ij}$ be the daily minimum temperature on day i in period j and let TN $_{in}10$ be the calendar day 10th percentile centred on a 5-day window for the base period 1971–2000. The percentage of time for the base period is determined where TN $_{ij} < TN_{in}10$	Reference period changed from 1961–1990 to 1971–2000	%
TX10 p (Cool days)	Percentage of days when daily maximum temperature < 10th percentile: Let TX $_{ij}$ be the daily maximum temperature on day i in period j and let TX $_{in}10$ be the calendar day 10th percentile centred on a 5-day window for the base period 1971–2000. The percentage of time for the base period is determined where TX $_{ij} < TX_{in}10$	Reference period changed from 1961–1990 to 1971–2000	%
TN90 p (Warm nights)	Percentage of days when daily minimum temperature > 90th percentile: Let TN $_{ij}$ be the daily minimum temperature on day i in period j and let TN $_{in}90$ be the calendar day 90th percentile centred on a 5-day window for the base period 1971–2000. The percentage of time for the base period is determined where TN $_{ij} > TN_{in}90$	Reference period changed from 1961–1990 to 1971–2000	%
TX90 p (Warm days)	Percentage of days when daily maximum temperature > 90th percentile: Let TX $_{ij}$ be the daily maximum temperature on day i in period j and let TX $_{in}90$ be the calendar day 90th percentile centred on a 5-day window for the base period 1971–2000. The percentage of time for the base period is determined where TX $_{ij} > TX_{in}90$	Reference period changed from 1961–1990 to 1971–2000	%

WSDI (Warm spell duration index)	Annual count of days with at least 6 consecutive days when daily maximum temperature > 90th percentile: Let TX_{ij} be the daily maximum temperature on day i in period j and let TX_{in90} be the calendar day 90th percentile centred on a 5-day window for the base period 1971–2000. Then, the number of days per period is summed where, in intervals of at least 6 consecutive days, $TX_{ij} > TX_{in90}$	Reference period changed from 1961–1990 to 1971–2000	Day
CSDI (Cold spell duration index)	Annual count of days with at least 6 consecutive days when daily minimum temperature < 10th percentile: Let TN_{ij} be the daily minimum temperature on day i in period j and let TN_{in10} be the calendar day 10th percentile centred on a 5-day window for the base period 1971–2000. Then, the number of days per period is summed where, in intervals of at least 6 consecutive days, $TN_{ij} < TN_{in10}$	Reference period changed from 1961–1990 to 1971–2000	Day

REFERENCES

- Arnfield, A. J., 2003: Two decades of urban climate research: A review of turbulence, exchanges of energy and water, and the urban heat island. *Int. J. Climatol.*, **23**, 1–26.
- Bornstein, R. D., 1968: Observations of the urban heat island effect in New York city. *J. Appl. Meteor.*, **7**, 575–582.
- Chan Ho-sun, Lee Tsz-cheung, and Ginn Wing-lui, 2010: Performance of IPCC AR4 climate models in simulating the temperature over southern China. The 24th Guangdong-Hong Kong-Macao Seminar on Meteorological Science and Technology, Shenzhen, China, 20–22 January 2010. Hong Kong Observatory Reprint No. 856, 10 pp. (in Chinese).
- Census and Statistics Department, 2007: Hong Kong Population Projections 2007–2036. <http://www.censtatd.gov.hk/freedownload.jsp?file=publication/stat-report/population/B1120015032007XXXXB0200.pdf&title=Hong+Kong+Population+Projections+2007-2036>.
- Cheng, C. S., G. Li, Q. Li, and H. Auld, 2008: Statistical downscaling of hourly and daily climate scenarios for various meteorological variables in South-Central Canada. *Theor. Appl. Climatol.*, **91**, 129–147.
- Crawley, M. J., 2008: *The R Book*. John Wiley & Sons, Ltd. Chichester, West Sussex, English, 942 pp.
- Coles, S. G., 2001: *An Introduction to Statistical Modeling of Extreme Values*. Springer-Verlag, London, 208 pp.
- Fan Li-jun, Fu Cong-bin, and Chen De-liang, 2005: Review on creating future climate change scenarios by statistical techniques. *Adv. Earth Sci.*, **20**, 320–329. (in Chinese)
- Fowler, H. J., and M. Ekström, 2009: Multi-model ensemble estimates of climate change impacts on UK seasonal precipitation extremes. *Int. J. Climatol.*, **29**, 385–416.
- Fong, S. K., C. H. Wu, A. Wang, Z. J. He, T. Wang, K. C. Leong, and U. M. Lai, 2009: Analysis of surface air temperature change in Macau during 1901–2007. *Advances in Climate Change Research*, **5**(1), 12–17.
- Frich, P., L. V. Alexander, P. Della-Marta, B. Gleason, M. Haylock, A. M. G. Klein Tank, and T. Peterson, 2002: Observed coherent changes in climate extremes during the second half of the 20th century. *Climate Res.*, **19**, 193–212.
- Guangdong Provincial Meteorological Bureau, 2007: Assessment report on climate change of Guangdong (Selection). *Guangdong Meteorology*, **29**(3), 1–14.
- HKO, 2009: Weather forecast description. <http://www.hko.gov.hk/wxinfo/currwx/flw-description/flw-e.htm#0101>.
- Houghton, J. T., 2009: *Global Warming: The Complete Briefing*. Cambridge University Press, Cambridge, UK, 438 pp.
- Huth, R., 1999: Statistical downscaling in central Europe: Evaluation of methods and potential predictors. *Climate Res.*, **13**, 91–101.
- IPCC, 2007a: Climate Change 2007: The Physical Science Basis. Contribution of the Working Group I to the Fourth Assessment Report of the Intergovernmental Panel on Climate Change. Solomon, S., D. Qin, M. Manning, Z. Chen, M. Marquis, K. B. Averyt, M. Tignor and H. L. Miller, Eds. Cambridge University Press, Cambridge, United Kingdom and New York, NY, USA, 996 pp.

- IPCC, 2007b: Summary for Policymakers. In: *Climate Change 2007: Impacts, Adaptation and Vulnerability. Contribution of Working Group II to the Fourth Assessment Report of the Intergovernmental Panel on Climate Change*. M. L. Parry, O. F. Canziani, J. P. Palutikof, P. J. van der Linden and C. E. Hanson, Eds., Cambridge University Press, Cambridge, UK, 7–22.
- Kalnay, E., and M. Cai, 2003: Impact of urbanization and land-use change on climate. *Nature*, **423**, 528–531.
- Karl, T. R., W. C. Wang, M. E. Schlesinger, R. W. Knight, and D. Portman, 1990: A method of relating general circulation model simulated climate to the observed local climate. Part I: Seasonal statistics. *J. Climate*, **3**, 1053–1079.
- , H. F. Diaz, and G. Kukla, 1988: Urbanization: its detection and effect in the United States climate record. *J. Climate*, **11**, 1099–1123.
- Kharin, V. V., and F. W. Zwiers, 2005: Estimating extremes in transient climate change simulations. *J. Climate*, **18**, 1156–1173.
- Kiktev, D., J. Caesar, L.V. Alexander, H. Shiogama, and M. Collier, 2007: Comparison of observed and multimodeled trends in annual extremes of temperature and precipitation. *Geophys. Res. Lett.*, **34**, L10702, doi:10.1029/2007GL029539.
- Kilsby, C. G., P. S. P. Cowpertwit, P. E. O’connell, and P. D. Jones, 1998: Predicting rainfall statistics in England and Wales using atmospheric circulation variables. *Int. J. Climatol.*, **18**, 523–539.
- Knutti, R., 2008: Should we believe model predictions of future climate change? *Phil. Trans. R. Soc. A*, **366**, 4647–4664, doi: 10.1098/rsta.2008.0169.
- Lee, T. C., W. M. Leung, and K. W. Chan, 2006: Climatological normals for Hong Kong 1971–2000. Hong Kong Observatory Technical Note (Local) 83, 31 pp.
- , H. S. Chan, E. W. L. Ginn, and M. C. Wong, 2011: Long-term trends in extreme temperatures in Hong Kong and southern China. *Adv. Atmos. Sci.*, **28**(1), 147–157.
- Leung, Y. K., K. H. Yeung, E. W. L. Ginn, and W. M. Leung, 2004a: Climate Change in Hong Kong. Hong Kong Observatory Technical Note 107, 41 pp.
- , E. W. L. Ginn, M. C. Wu, K. H. Yeung, and W. L. Chang, 2004b: Temperature projections for Hong Kong in the 21st century. *Bull. H. K. Meteor. Soc.*, **14**(1/2), 21–48.
- , M. C. Wu, K. K. Yeung, and W. M. Leung, 2007: Temperature projections in Hong Kong based on IPCC Fourth Assessment Report. *Bull. H. K. Meteor. Soc.*, **17**, 13–22.
- , K. M. Yip, and K. H. Yeung, 2008: Relationship between thermal index and mortality in Hong Kong. *Meteorological Applications*, **15**(3), 399–409.
- Meehl, G. A., F. Zwiers, J. Evans, T. Knutson, L. Mearns, and P. Whetton, 2000: Trends in extreme weather and climate events: Issues related to modeling extremes in projections of future climate change. *Bull. Amer. Meteor. Soc.*, **81**(3), 427–436.
- , and C. Tebaldi, 2004: More intense, more frequent, and longer lasting heat waves in the 21st century. *Science*, **305**(5686), 994–997, doi: 10.1126/science.1098704.
- , and K. A. Hibbard, 2007: A strategy for climate change stabilization experiments with AOGCMs and ESMs. WCRP Informal Report No. 3/2007, ICPO Publication No. 112, IGBP Report No. 57, World Climate Research Programme, Geneva, 35 pp.
- Mitchell, J. F. B., J. Lowe, R. A. Wood, and M. Vellinga, 2006: Extreme events due to human-induced climate change. *Philos. T. Roy. Soc. A*, **364**, 2117–2133.
- Murphy, J. M., 1999: An evaluation of statistical and dynamical techniques for downscaling local climate. *J. Climate*, **12**, 2256–2284.
- Nakicenovic, N., J. Alcamo, G. Davis, B. de Vries, J. Fenhann, S. Gaffin, K. Gregory, A. Grubler, T. Y. Jung, T. Kram, E. L. La Rovere, L. Michaelis, S. Mori, T. Mordsita, W. Pepper, H. Pitcher, L. Price, K. Raihi, A. Roehrl, H.-H. Rogner, A. Sankovski, M. Schlesinger, P. Shukla, S. Smith, R. Swart, S. van Rooijen, N. Victor, and Z. Dadi, 2000: *IPCC Special Report on Emissions Scenarios*. Cambridge University Press, Cambridge, United Kingdom and New York, NY, USA, 599 pp.
- Oke, T. R., 1973: City size and the urban heat island. *Atmos. Environ.*, **7**, 769–779.
- , 1982: The energetic basis of the urban heat island. *Quart. J. Roy. Meteor. Soc.*, **108**, 1–24.
- Pancura, M., and G. S. Lines, 2005: Variability and Extremes in Statistically Downscaled Climate Change Projections at Greenwood Nova Scotia. Meteorological Service of Canada, Atlantic Region Science Report Series 2005-10, October 2005, 35 pp.
- Peterson, P., 1981: Extreme Temperatures in Hong Kong. Hong Kong Observatory Technical Note (Local) 22, 35 pp.

- Peterson, T. C., and Coauthors, 2001: Report on the Activities of the Working Group on Climate Change Detection and Related Rapporteurs 1998–2001. WMO, Rep. WCDMP-47, WMO-TD 1071, Geneva, Switzerland, 143 pp.
- , 2005: Climate change indices. *WMO Bulletin*, **54**(2), 83–86.
- Reifen, C., and R. Toumi, 2009: Climate projections: Past performance no guarantee of future skill. *Geophys. Res. Lett.*, **36**, L13704, doi:10.1029/2009GL038082.
- Schubert, S., 1998: Downscaling local extreme temperature changes in southeastern Australia from the CSIRO Mark2 GCM. *Int. J. Climatol.*, **18**, 1419–1438.
- STARDEX, 2005: STARDEX Final Report–Downscaling Climate Extremes, EU. http://www.cru.uea.ac.uk/projects/stardex/reports/STARDEX_FINAL_REPORT.pdf.
- Sterl, A., C. Severijns, H. Dijkstra, W. Hazeleger, G. Jan van Oldenborgh, M. van den Broeke, G. Burgers, B. van den Hurk, P. Jan van Leeuwen, and P. van Velthoven, 2008: When can we expect extremely high surface temperatures? *Geophys. Res. Lett.*, **35**, L14703, doi:10.1029/2008GL034071.
- Torok, S. J., C. J. G. Morris, C. Skinner, and N. Plummer, 2001: Urban heat island features of Southeast Australian towns. *Aust. Met. Mag.*, **50**, 1–13.
- Wilby, R. L., S. P. Charles, E. Zorita, B. Timbal, P. Whetton, and L. Mearns, 2004: Guidelines for Use of Climate Scenarios Developed from Statistical Downscaling Methods. 27 pp.
- Wild, H., A. Ohmura, and K. Makowski, 2007: Impact of global dimming and brightening on global warming. *Geophys. Res. Lett.*, **34**, L04702, doi:10.1029/2006GL028031.
- Wilks, D. S., 2006: *Statistical Methods in the Atmospheric Sciences*. 2nd Edition, Academic Press. London, UK, 627 pp.
- WMO, 2009: Guidelines on Analysis of Extremes in a Changing Climate in Support of Informed Decisions for Adaptation. Climate Data and Monitoring WCDMP-No.72, 52 pp.
- Wong, M. C., and H. Y. Mok, 2009: Trends in Hong Kong climate parameters relevant to engineering design. HKIE Civil Division Conference 2009: Conference on Engineers' Responses to Climate Change, HKO Reprint No. 832, 30 pp.
- Xu Chong-hai, Shen Xin-yong, and Xu Ying, 2007: An analysis of climate change in East Asia by using the IPCC AR4 simulations. *Adv. Clim. Change Res.*, **3**(5), 287–292. (in Chinese)
- Yang, S., K. M. Lau, and K. M. Liu, 2002: Variations of the East Asian jet stream and Asian-Pacific American winter climate anomalies. *J. Climate*, **15**, 306–325.
- Zhang, D. F., A. S. Zakey, X. J. Gao, F. Giorgi, and F. Solmon, 2009, Simulation of dust aerosol and its regional feedbacks over East Asia using a regional climate model. *Atmos. Chem. Phys.*, **9**, 1095–1110.
- Zhou, K. M., R. E. Dickinson, Y. H. Tian, J. Y. Fang, Q. Z. Li, R. K. Kaufmann, C. J. Tucker, and R. B. Myneni, 2004: Evidence for a significant urbanization effect on climate in China. *Proceedings of the National Academy of Sciences*, **101**(26), 9540–9544.